^{13}C Relaxation Studies of the DNA Target Sequence for *Hha*I Methyltransferase Reveal Unique Motional Properties[†]

Zahra Shajani[‡,▽] and Gabriele Varani*[,‡,§]

Departments of Chemistry and Biochemistry, University of Washington, Seattle, Washington 98195-1700

Received October 11, 2007; Revised Manuscript Received April 28, 2008

ABSTRACT: The goal of this work was to examine if sequence-dependent conformational flexibility in DNA plays a role in base extrusion, a common conformational change induced by many DNA-modifying enzymes. We studied the dynamics of the double-stranded DNA target of the *Hha*I methyltransferase by recording an extensive set of ^{13}C NMR relaxation parameters. We observe that the cytidine furanose rings experience fast (picosecond to nanosecond) motions that are not present in other nucleotides; the methylation site experiences particularly high mobility. We also observe that the bases of guanosine and cytidine residues within the *Hha*I recognition sequence GCGC experience motions on a much slower (1−100 μs) time scale. We compare these observations with previous solution and solid-state NMR studies of the *Eco*RI nuclease target sequence, and solid-state NMR studies of a similar *Hha*I target construct. While an increased mobility of cytidine furanose rings compared to those of other nucleotides is observed for both sequences, the slower motions are only observed in the *Hha*I target DNA. We propose that this inherent flexibility lowers the energetic barriers that must occur when the DNA binds to the *Hha*I methyltransferase and for extrusion of the cytidine prior to its methylation.

Methylation of DNA is an important step in a host of biological processes, ranging from gene silencing to X-chromosome inactivation (*1*). The methyltransferase modification enzymes attach methyl groups to either the N4 or C5 position within the cytosine or the N6 position within adenine. The chemical addition of a methyl group to DNA bases is carried out by restriction−modification systems comprising a methyltransferase (Mtase) which methylates the DNA at specific recognition sites and an endonuclease (*2*).

Among the best studied methylation systems is *Hha*I[1] (*Haemophilius hemolyticus*), which is part of a defense mechanism in these bacteria that protects the cell form invasive foreign DNA. The *Hha*I system is comprised of the two canonical enzymes, the methyltransferase and endonuclease, where the former is expressed first and methylates the native DNA. The endonuclease is subsequently expressed and cleaves all nonmethylated foreign DNA. Both proteins recognize the sequence 5′-G↓CGC-3′ (the arrow indicates cleavage, and the underlined cytosine base is the methylation target). The covalent addition of a methyl group to the C5 position of the target cytosine inhibits endonucleolytic cleavage, protecting the bacterial DNA from its own endonuclease.

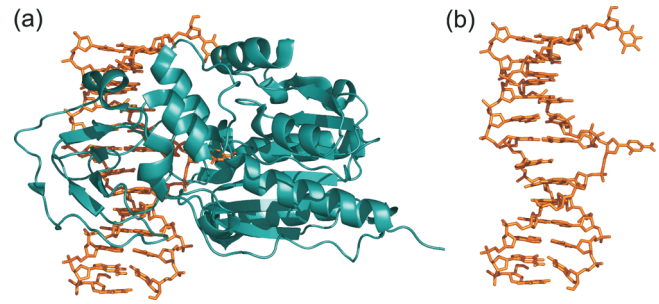

FIGURE 1: Structure of DNA−*Hha*I methyltransferase complex (Protein Data Bank entry 1FJX). (a) DNA−protein complex, in which the C6 base flips out ~170° in the presence of the methyltransferase. (b) Target DNA with the methyltransferase protein removed for clarity.

The methyltransferase DNA target forms a classical double helix, providing little access to the cytidine position to be methylated. However, the crystal structure of the *Hha*I Mtase complexed with its cognate double-stranded DNA (dsDNA) and methyl donor cofactor *S*-adenosyl-L-methionine (AdoMet) showed that the cytosine becomes exohelical in complex with the methylase and becomes surrounded by residues within the enzyme active site (Figure 1) (*3*). Thus, the physical removal from the conformation observed in the B-form helix explains how the cytosine C5 position becomes accessible to the enzyme. However, it is still unclear how the methylase extrudes the base from the double helix, either by actively inducing base flipping or by more passively capturing a transient conformation where the base is at least partially extended outside of the helix.

[†] Supported by NIH Grant RO1 EB003152.

* To whom correspondence should be addressed. E-mail: varani@chem.washington.edu. Telephone: (206) 543-7113. Fax: (206) 685-8665.

[‡] Department of Chemistry.

[▽] Present address. The Scripps Research Institute, Department of Molecular Biology, 10550 N. Torrey Pines, La Jolla, CA 92037.

[§] Department of Biochemistry.

[1] Abbreviations: AdoMet, *S*-adenosyl-L-methionine; CSA, chemical shielding anisotropy; *Hha*I, *Haemophilius hemolyticus*; HSQC, heteronuclear single-quantum correlation spectroscopy; T_1, longitudinal relaxation time; $T_{1\rho}$, rotating frame relaxation time; NOE, nuclear Overhauser effect.

10.1021/bi7020469 CCC: $40.75
Published on Web 06/26/2008

Earlier work has found that mutation of the target C to A, T, G, U, or m5C leads to the formation of stable DNA−protein complexes (*4*) and suggests that these complexes have flipped-out bases. Crystal structures demonstrated that when the target C base is mutated so that G:A, G:U, and G:AP (where AP is an abasic site) mismatch pairs are formed, the mismatched adenine and uracil are all flipped out into the enzyme active site pocket as in the cognate sequence (*5*). In the case of a G:AP mismatch, conformational changes occur in the target abasic nucleotide similar to those that effect base flipping, yet deleting any nucleotide in the recognition site from a position other than the target site leads to a loss of interaction with the methylase (*4, 6*). Thus, the identity of the extruded nucleotide is not important, yet base flipping is sequence specific. These observations suggested that the interaction between M.*Hha*I and the target DNA is not characterized solely by specific interactions between protein residues and specific positions on the target base but that recognition also requires interactions with the nonmethylated base pairs when the target base is correctly positioned (*4*).

We have previously hypothesized that motions specific to the *Hha*I target sequence facilitate base extrusion by this enzyme, thereby making base flipping energetically feasible. Consistent with this hypothesis, solid-state NMR work has shown considerable sequence-dependent dynamics, on a microsecond to nanosecond time scale, across the four nucleotides recognized by the methylase (*7*). ^{19}F NMR has been used in the past to characterize the solution-state motions within the cytosine that is the target for methylation, but these studies were limited because a single probe of dynamics was used (*8*). To probe more extensively the motional characteristics of this DNA sequence in solution, we used ^{13}C NMR relaxation to study base and sugar dynamics for the DNA target of *Hha*I methyltransferase.

In this work, we report ^{13}C T_1, $T_{1\rho}$, and heteronuclear NOE values for sugar and base nuclei and the analysis of the motional properties of the *Hha*I DNA based on the model-free formalism (*9–11*). Surprisingly, we found significant differences in the relaxation properties of the furanose rings of cytosines that are distinct from those observed for the other bases and much slower motions for the bases within the *Hha*I recognition sequence. To investigate whether the motions we observed are specific to the *Hha*I target sequence, we compare our work to solution (*11*) and solid-state NMR studies of the *Eco*RI DNA target (*12–15*), and to solid-state NMR studies of a similar construct of the *Hha*I DNA target (*7*). In both sequences, the furanose rings of the deoxycytidines have increased mobility compared to the other nucleotides, although the *Hha*I methylation site remains particularly flexible. In contrast, the slower (1−100 μs) motions observed for bases within the *Hha*I target sequence are not evident in the *Eco*RI target DNA (*16*).

EXPERIMENTAL PROCEDURES

DNA Preparation. A uniformly ^{13}C- and ^{15}N-labeled non-palindromic dsDNA dodecamer with the sequence [5′-(dGGTAGCGCTATT)-3′]-[5′-(dAATAGCGCTACC)-3′] (Figure 2) was purchased from BioQuantis. Each strand of DNA was dissolved and dialyzed into NMR buffer [10 mM potassium phosphate buffer, 50 mM KCl, and 0.1 mM EDTA (pH 6.0)]. After lyophilization, each strand was redissolved in 99.9% D_2O, lyophilized again, and finally dissolved in 99.99% D_2O, to remove any residual water. The two strands were combined, heated to 90 °C, and snap-cooled. The final sample concentration was 1.3 mM dsDNA.

FIGURE 2: Sequence of the *Hha*I target DNA. The recognition sequence is colored blue with the methylation site underlined.

To demonstrate that the desired duplex was formed with a 1:1 stoichiometry, ^{13}C HSQC experiments were performed first on the single-stranded DNAs. Each single strand yielded 24 resonances for the C6/C8 region at 25 °C, suggesting the formation of multiple conformations, probably a duplex in equilibrium with the single strands for these partially complementary sequences. However, at 45 °C, only 12 resonances could be seen in the C6/C8 region for each of the individual strands, suggesting that a single conformer could easily be formed by thermal denaturation. Indeed, when the two strands were annealed at 25 °C, 16 resonances were found, as expected for the desired duplex with no alternate conformers.

Spectral Assignments. Proton and carbon assignments for the double-stranded DNA were obtained from the analysis of two-dimensional (2D) NOESY and three-dimensional (3D) ^{13}C NOESY-HSQC spectra recorded in 99.9% D_2O at 25 °C using a Bruker Avance-500 spectrometer. Spectral assignments were based on standard NMR methods (*17*). A 2D NOESY spectrum collected with a mixing time of 200 ms was analyzed to generate initial proton assignments. The 3D ^{13}C NOESY-HSQC experiment (mixing time of 120 ms) was then used to assign the carbon resonances.

NMR Relaxation Experiments. T_1, $T_{1\rho}$, and heteronuclear NOE values were recorded as a series of 2D NMR spectra, in which the relaxation delay τ was parametrically increased. All experiments were performed in the constant-time mode. Data collection was performed on a Bruker Avance-500 instrument on the same 1.3 mM sample of DNA in 99.9% D_2O at 25 °C. Data were collected on a TXI triple-resonance HCN probe. ^{15}N or ^{31}P decoupling was not introduced to reduce sample heating.

The constant time delays were set to 7.15 and 12.5 ms when base and sugar relaxation properties were recorded, respectively, corresponding to ^{13}C−^{13}C coupling constants of approximately 70 Hz (bases) and 40 Hz (sugars) (*18*). The relaxation delay between scans was set to 1.9 s. Spectra were recorded with 86 complex points (base resonances) and 128 complex points (sugars) in the indirect dimension. The total collection time for each set of experiments was ~24 h for either T_1 or $T_{1\rho}$ measurements.

Selective excitation was accomplished by application of ^{13}C 180° IBURP-shaped pulses during the first INEPT transfer (*11, 19*). An inversion bandwidth of 8 ppm was achieved by using pulses with a duration of 1 s at a ^{13}C frequency of 125 MHz. The C6 and C5 resonances are separated by 40 ppm, enabling T_1 to be easily measured for either nucleus without excitation of the other through the use of these selective pulses. Unlike in RNA, the ribose resonances are well dispersed in DNA and selective excita-

tion is possible for C1′, C2′ (H′ and H″), C3′, C4′, and C5′ (H′ and H″) nuclei. Each spectral region required collection of an independent set of T_1 values to ensure selectivity, whereas for $T_{1\rho}$ and NOE experiments, data for the C1′/C4′ and C3′/C5′ regions could be collected together. ^{13}C T_1 relaxation data were collected for the C8 resonances using nonselective pulses by setting the carrier frequency to 141 ppm. Using selective excitation pulses, ^{13}C T_1 relaxation data were collected for the C6 region in the bases (at 141 ppm), C1′ (carrier set to 91.5 ppm), C2′ (carrier set to 43 ppm), C3′ (carrier set to 60 ppm), and C5′/C5″ (carrier set to 69 ppm) in the sugar. For $T_{1\rho}$ and NOE experiments, relaxation data were collected for C8 and C6 resonances (carrier set to 141 ppm), C1′ (carrier at 91.5 ppm), C2′ ($T_{1\rho}$ only, carrier set to 43 ppm), and C3′/C5′/C5″ (carrier set to 69 ppm).

$T_{1\rho}$ experiments were executed at a spin-lock field of 2 kHz. Delays of 5, 20, 40, 80, 120, 160, 240, 320, 500, 600, and 760 ms and 8, 12, 20, 40, 60, 80, and 96 ms were used for T_1 and $T_{1\rho}$ experiments, respectively. One of the experimental points at random was repeated in a triplicate manner for each run to test the reproducibility of the measurements. For heteronuclear NOE measurements, a pair of spectra were recorded, one with initial proton saturation and one without. Proton saturation was achieved by the application of a train of 120° ^1H pulses applied each 5 ms. Spectra recorded with proton saturation utilized a relaxation delay of 2.5 s followed by a 2.5 s period of saturation. Spectra recorded in the absence of saturation employed a total recycle delay of 5 s. Heteronuclear NOE spectra were collected at 11.7 T for all the base and sugar resonances.

Power Dependence of $T_{1\rho}$. Data reporting on the power dependence of $T_{1\rho}$ were collected and analyzed for C8−H8 and C6−H6 resonances at 11.7 T as a series of $T_{1\rho}$ experiments at various spin-lock field strengths (1.2, 2.6, 3.6, and 6.6 kHz). These values were set by modifying the power level of the spin-lock pulse. Data at each power level were collected and analyzed independently with the same settings and delays as described above for collection of $T_{1\rho}$ data. For the higher spin-lock fields (3.6 and 6.6 kHz), the longest relaxation delay was set to 28 ms to avoid sample heating.

Data Analysis. All data were processed as described previously (*20, 21*). Briefly, T_1 and $T_{1\rho}$ were determined from the decay curves using the standard equation

$$I(\tau) = I_o \exp(-\tau/T_{1/1\rho}) \quad (1)$$

where I_o is the initial peak intensity and τ is the delay time. The errors for the rate constants were estimated by Sparky and reflect the likely errors of the best fit $T_{1/1\rho}$ from the $T_{1/1\rho}$ values obtained for a perfect exponential decay; error estimates are reported in the Results. The heteronuclear NOE values were calculated from the ratio of the intensity of saturated to unsaturated spectra. Uncertainties in these measurements were estimated from the base plane noise in the 2D $^1H-^{13}C$ HSQC spectra recorded with and without proton saturation, as described previously (*22*). Relaxation times were derived using all time delays mentioned above; reassuringly, the results did not change by more than 2% when only the first six delay points were fitted, indicating that relaxation is monoexponential. Thus, cross-talk between neighboring ^{13}C nuclei is effectively minimized by the use of selective excitation pulses (*11*).

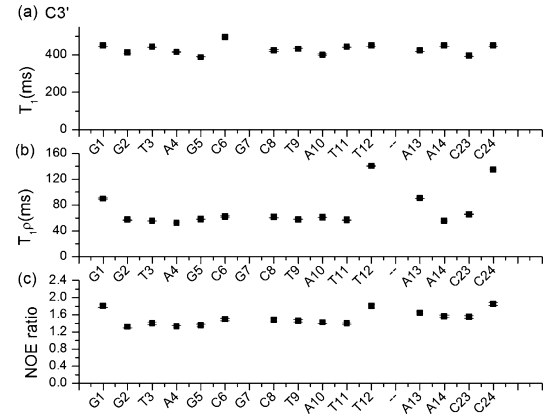

FIGURE 3: Relaxation times for C3′−H3′ spins: (a) ^{13}C T_1, (b) ^{13}C $T_{1\rho}$, and (c) heteronuclear NOE. Residues that had noisy relaxation curves or that were partially or completely overlapped were excluded from the analysis.

Analysis of Relaxation Data with the Modelfree Approximation. Quantitative analysis of the base (C8−H8 and C6−H6 resonances) and sugar C1′−H1′ and C3′−H3′ relaxation data was conducted using the model-free approximation (*9, 10*) with the program ModelFree 4.15 (*23*) in a manner analogous to previous studies of RNA (*20, 24*). Model selection was conducted according to previously reported procedures (*23, 25*). Due to additional relaxation mechanisms between the strong coupled H2′ and H2″ nuclei, the C2′−H2′ resonances were not analyzed quantitatively. The rotational correlation time for the entire molecule was found to be 4 ns for all models with a D_{ratio} of 2.0 and C−H bond lengths of 1.09 and 1.104 Å for the ribose and bases, respectively.

For this analysis, we used the values of chemical shift anisotropies (CSAs) that were recently reported for double-stranded B-form DNA (144 ppm for dA-C8, 133 ppm for dG-C8, 168 ppm for dT-C6, and 186 ppm for dC-C6) for the base resonances (*26*). These CSA values also agree well with those determined by solid-state NMR on DNA mononucleosides (*27*). The CSA used for ribose resonances was 30 ppm, as determined by Bryce and co-workers (*28*) and Stueber and Grant (*27*).

For the C1′−H1′ resonances, three resonances were fit to model 2 (T9, T11, and A14), eight resonances to model 5 (G1, T3, A4, G7, C8, A10, T12, and A13), and the remaining five resonances (G2, G5, C6, C23, and C24) to model 4. For the C3′−H3′ resonances, one resonance was fit to model 2 (A13) and two resonances were fit to model 5 (T12 and C24); the remaining residues were fit to model 4. However, it was not possible to fit the base resonances, likely because many of them exhibited exchange (see below).

RESULTS

Data Collection and Analysis. ^{13}C T_1, $T_{1\rho}$, and heteronuclear NOE values were recorded as described in Experimental Procedures. All relaxation decay curves could be fit very well by single exponentials, without any evidence of multiexponential behavior, suggesting that cross-talk between neighboring spins was minimized by the use of selective excitation pulses. The observed relaxation times obtained from the analysis of these decay curves and the heteronuclear NOEs measured at 11.7 T are shown in Figures 3–6. This

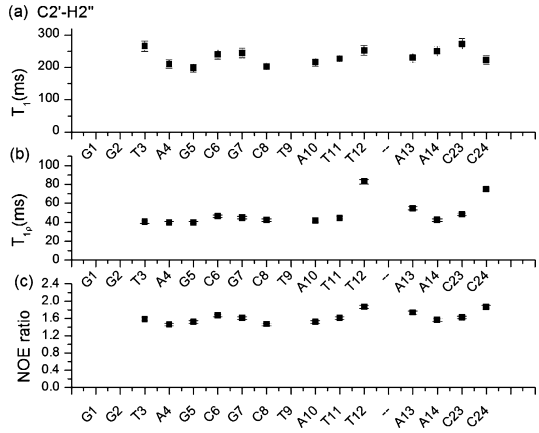

FIGURE 4: Relaxation times for C2′−H2″ spins: (a) ^{13}C T_1, (b) ^{13}C $T_{1\rho}$, and (c) heteronuclear NOE. Residues that had noisy relaxation curves or that were partially or completely overlapped were excluded from the analysis.

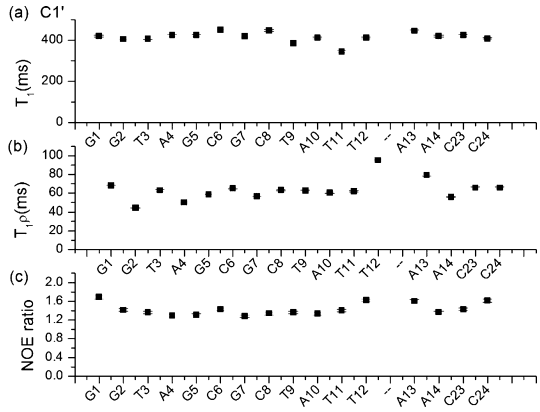

FIGURE 5: Relaxation times for C1′−H1′ spins: (a) ^{13}C T_1, (b) ^{13}C $T_{1\rho}$, and (c) heteronuclear NOE. Residues that had noisy relaxation curves or that were partially or completely overlapped were excluded from the analysis.

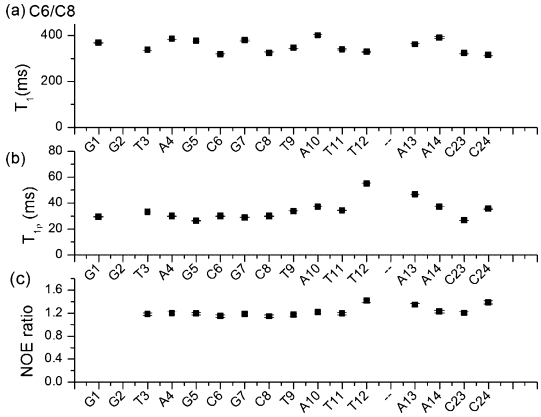

FIGURE 6: Relaxation times for C6−H6 and C8−H8 spins: (a) ^{13}C T_1, (b) ^{13}C $T_{1\rho}$, and (c) heteronuclear NOE. Residues that had noisy relaxation curves or that were partially or completely overlapped were excluded from the analysis.

field was chosen to minimize artifacts in the analysis arising from the noncollinearity of the CSA with the C−H bond and the large CSA of base nuclei (*20, 29*).

Chemical shift assignments were obtained using standard methods based on the analysis of 2D NOESY and 3D ^{13}C-edited NOESY-HSQC spectra; assignments have been deposited into the BioMagResBank. Some nuclei were excluded from the analysis of the relaxation data because

Table 1: Average Relaxation Times and NOE Ratios for Ribose Resonances (excluding 5′ and 3′ terminal residues)

	T_1 (ms)	$T_{1\rho}$ (ms)	NOE ratio
C1′−H1′	413 (0.8%)	59 (0.6%)	1.36 (2%)
C2′−H2′	151 (9.7%)	42 (2.4%)	1.57 (2%)
C2′−H2″	233 (6%)	42 (2.4%)	1.55 (2%)
C3′−H3′	424 (1.0%)	59 (1.0%)	1.40 (2%)
C4′−H4′	410 (0.8%)	57 (0.8%)	1.38 (2%)

Table 2: Average Relaxation Times and NOE Ratios for Base Resonances (excluding 5′ and 3′ terminal residues)

	T_1 (ms)	$T_{1\rho}$ (ms)	NOE ratio
A: C8−H8	392 (0.9%)	35 (0.9%)	1.22 (1.8%)
G: C8−H8	379 (0.9%)	28 (0.9%)	1.19 (1.8%)
T: C6−H6	341 (1.1%)	34 (0.7%)	1.18 (1.8%)
C: C6−H6	322 (1.1%)	29 (0.7%)	1.17 (1.8%)

the corresponding resonances were overlapped. However, the ^{13}C relaxation properties for six of eight purine C8, all of the pyrimidine C6 (eight of eight), and all ribose C1′ (16 of 16) resonances could be measured and analyzed reliably. The ^{13}C relaxation properties of 13 of 16 C2′−H2′ and C2′−H2″ peaks and 14 of 16 C3′−H3′ peaks could also be measured and analyzed. Unfortunately, most of the resonances in the C5′−H5′ and C5−H5″ region were overlapped and could not be resolved sufficiently well to warrant analysis.

Qualitative Analysis of the ^{13}C Relaxation Data. The average relaxation rates are reported first, since they provide a reference point for establishing which residues deviate from the behavior expected for a perfectly rigid duplex (Tables 1 and 2). The data demonstrate the presence of noticeably less restricted motions at the ends of the sequence, which is expected as the terminal bases fray in solution. The $T_{1\rho}$ and NOE values are substantially larger than the average observed in the rest of the helix, suggesting the presence of extensive motions on the picosecond to nanosecond time scale. Thus, the 5′ and 3′ terminal residues were excluded from the averages listed in Tables 1 and 2 because of anomalous motional properties due to well-known end effects (base fraying).

More specifically, the C3′−H3′ resonances of the terminal G1 residue and C24 residues have $T_{1\rho}$ values that are 55 and 210% (90 and 135 ms, respectively) greater than average and NOE ratios that are 34 and 23% (1.80 and 1.85, respectively) greater than average, respectively. The terminal T12 and A13 residues have $T_{1\rho}$ values that are 250 and 57% (141 and 90 ms, respectively) greater than average and NOE values that are 27 and 14% (1.80 and 1.64, respectively) greater than average, respectively. Surprisingly, all the deoxycytidines (terminal residues are not considered in this analysis) have $T_{1\rho}$ values that are 8−12% and NOE values that are 5−12% larger compared to those of the deoxyadenosines, deoxyguanosines, and deoxythymidines, implying that the riboses of the deoxycytidines are somewhat more flexible on a picosecond to nanosecond time scale compared to the other nucleotides.

The C2′−H2″ resonance of C24 has a $T_{1\rho}$ value that is 66% (75 ms) greater than average and a NOE ratio that is 20% (1.86) greater than average. The T12 residue and A13 residue have $T_{1\rho}$ values that are 98% (83 ms) and 31% (54 ms) greater than average and NOE ratios that are 20% (1.86) and 12% (1.73) greater than average, respectively.

As with the C3′−H3′ resonances, the deoxycytidines (not considering terminal residues) have slightly larger $T_{1\rho}$ values (7%) than the deoxyadenosines, deoxyguanosines, and deoxythymidines.

For the C1′−H1′ resonances as well, the 5′ G-C and 3′ A-T pairs have larger $T_{1\rho}$ and NOE values, but to a lesser extent compared to the C2′−H2″ and C3′−H3′ resonances. This difference probably reflects the larger effect on C2′ and C3′ of the transition of the furanose ring between C2′- and C3′-endo conformers that is often observed for nucleotides at the 5′ and, especially, 3′ end of helices. Thus, the G1 residue has a $T_{1\rho}$ value that is 17% (68 ms) greater than average and a NOE ratio that is 25% (1.69) greater than average. The T12 and A13 residues have $T_{1\rho}$ values that are 53% (95 ms) and 43% (79 ms) greater than average and NOE values that are 18% (1.62) and 20% (1.60) larger, respectively. Unexpectedly, the average $T_{1\rho}$ values (again not considering the terminal residues) for both (deoxycytidine and deoxythymidine) are 12% higher than those of the purines. The increased flexibility of the C1′−H1′ deoxycytidines reflected in this anomalous relaxation rate is consistent with what is observed for other ribose carbons. Overall, these results suggest that the entire furanose ring of cytosines experiences increased motional freedom compared to the three other nucleotides.

As observed for the sugar rings, the base resonances of the 5′ and 3′ terminal residues also display anomalous dynamics, suggesting the presence of extensive motions on the picosecond to nanosecond time scale. The C6−H6 base resonance of the T12 residue has $T_{1\rho}$ and NOE values that are 61 and 20% (55 ms and 1.42, respectively) greater than average, respectively. The C8−H8 base resonance for the A13 residue has $T_{1\rho}$ and NOE values that are 34 and 11% (47 ms and 1.35, respectively) greater than average, respectively. The C8 base resonance for the G1 residues has a NOE value that is 20% (1.36) greater than average. The C6 resonance for the C24 residue has $T_{1\rho}$ and NOE values that are 20 and 190% (35 ms and 1.39, respectively) greater than average, respectively.

Analysis of the average transverse relaxation times for each type of base shows unexpected differences which are well beyond any experimental uncertainty (Table 2). Given the magnitude of the CSA, we would have predicted that the purine (G and A) bases would have very similar relaxation times if the DNA helix behaved as a perfectly rigid molecule without any significant internal motion, and the pyrimidine bases (T and C) would also have similar relaxation times. Instead, we observe that the G and C bases have average $T_{1\rho}$ relaxation times that are 20% smaller than those of the A and T bases. However, for each particular type of base, there are no large differences across the sequence among dA, dC, dG, and dT (excluding the terminal residues); i.e., C6, C8, and C23 all have similar values, with one significant exception. The A4 base residue has a $T_{1\rho}$ value (30 ms) lower than those of the other two A's (37 ms); interestingly, A4 is adjacent to the *Hha*I recognition sequence GCGC.

These differences in relaxation times cannot be attributed to the CSA or to anisotropic tumbling (see below) and reflect real differences in the internal dynamics of this DNA sequence. Interestingly, the longitudinal relaxation times do not follow this trend but rather behave as would be predicted from the relative values of the CSA, with the pyrimidine bases (which have the largest CSA) exhibiting the smallest T_1 values. This result strongly suggests that the differences in relaxation times between different nucleotides can be attributed to motions on time scales (microseconds to milliseconds) which affect only the transverse but not the longitudinal relaxation times.

Power Dependence of $T_{1\rho}$ for Base Resonances. The qualitative analysis of the previous paragraph attributed the reduction of dG and dC (as well as A4) base transverse relaxation times to motions on microsecond to millisecond time scales. To test this hypothesis, we measured the power dependence of $T_{1\rho}$. Resonances that exhibit conformational exchange on the time scale corresponding to the power of the spin-lock pulses will display a decrease in the relaxation rate as the spin-lock field strength increases. Consistent with our interpretation of the primary relaxation times, we observe a slight power dependence of $T_{1\rho}$ for all of the deoxycytidine resonances (Figure 7). This result demonstrates that the dC base residues are involved in conformational exchange processes, and the shape of the power dependence curves demonstrates that the rates of these processes are close to the microsecond time scale. Furthermore, G5 exhibited a strong initial dependence of relaxation rate on spin-lock power (Figure 7e) before leveling out, suggesting that motions occur at a rate that is at the edge of what can be probed with available power levels (e.g., 1−10 μs). These studies provide no evidence of conformational exchange processes for A4, G1, or G7, suggesting that the anomalous behavior of A4 and G7 may reflect motions on time scales that are too fast to be probed with current relaxation dispersion techniques.

ModelFree Analysis of the ^{13}C Relaxation Data. Quantitative analysis of the relaxation data using the model-free approximation was conducted with ModelFree 4.15 as described in Experimental Procedures. Data were best fit with an axially symmetric diffusion model, with a diffusion anisotropy of 2.0 and an overall correlation time (τ_m) of 4.0 ns. Appropriately, τ_m and the diffusion anisotropy were determined by excluding 5′ and 3′ terminal bases (because of an increased level of internal motion); this property was also calculated twice independently for C1′ and C3′ resonances with similar results to further validate the results. Previous studies on DNAs similar in size reported correlation times ranging from 3.3 to 5 ns (*16, 30*). A summary of the parameters that best describe the dynamics of each residue is given in Figure 8 and Table 3; errors for the order parameters are ~3% as determined with ModelFree 4.15. Residues that were fit best with model 4 required only low levels of R_{ex} (<4 ms^{-1}); we attributed this result simply to noise in the data (*20, 31*). Unfortunately, despite multiple attempts, the base residues could not be fit with ModelFree.

Consistent with the qualitative analysis of the relaxation times, we observe variations in the order parameters across the sequence. The C3′−H3′ resonances have an average S^2 value of 0.71 with a range of 0.57−0.83. The C1′−H1′ resonances have an average S^2 value of 0.78 and a range of 0.65−0.85. Reassuringly, this analysis shows increased flexibility (low values of S^2) for the ribose residues of the terminal residues, as expected from the qualitative inspection of the relaxation rates. From the C3′−H3′ data, the terminal residues (G1, T12, A13, and C24) have S^2 values of 0.49,

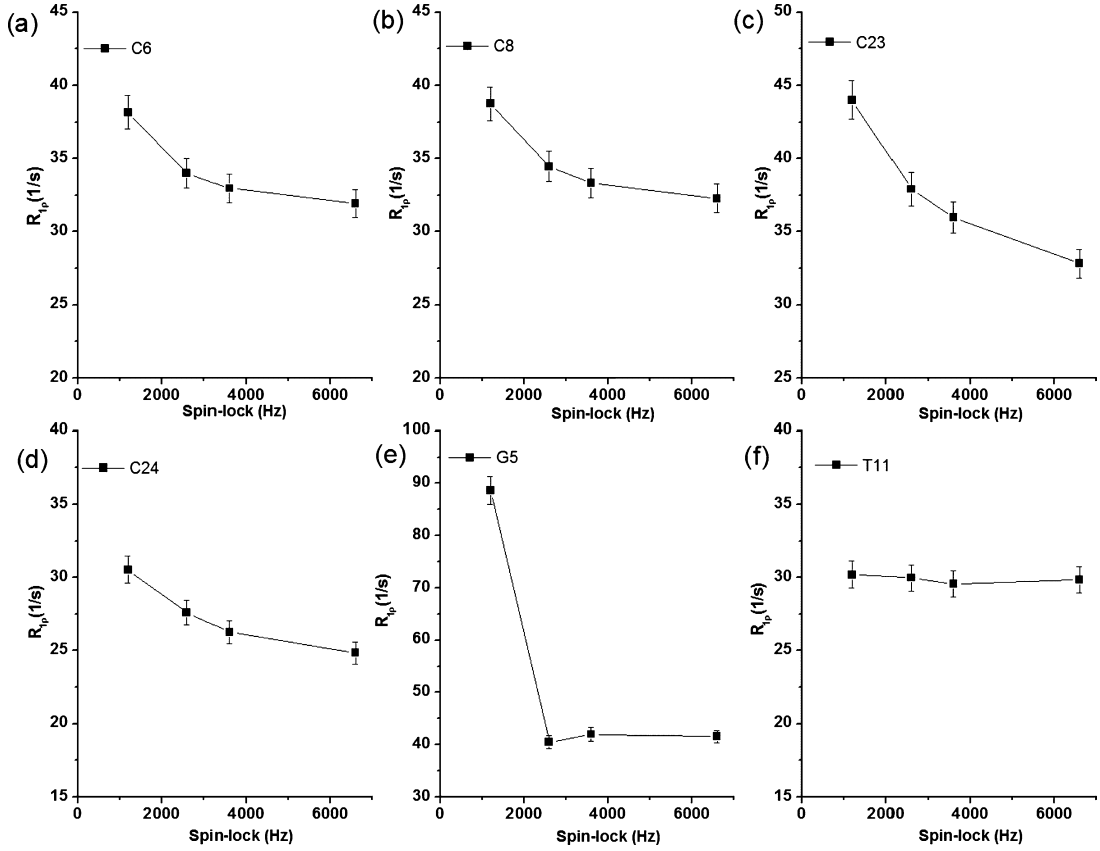

FIGURE 7: ^{13}C transverse relaxation rates ($R_{1\rho} = 1/T_{1\rho}$) vs applied spin-lock field strength (in hertz) at 500 MHz: (a) C6, (b) C8, (c) C23, (d) C24, (e) G5, and (f) T11 (this residue is shown as a reference for the case with no exchange).

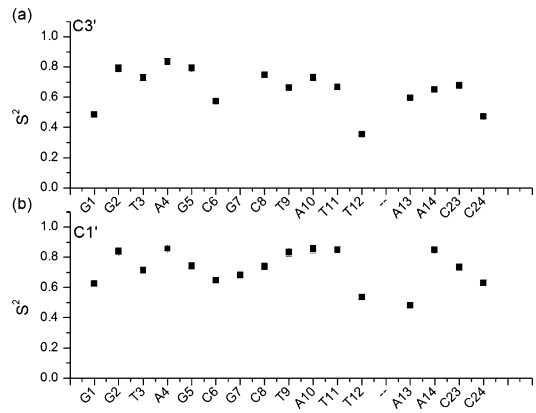

FIGURE 8: Order parameters (S^2) extracted from ModelFree analysis vs DNA sequence: (a) C3′ spins and (b) C1′ spins. Residues for which no results are shown correspond to overlapped cross-peaks or data that could not be fit with any ModelFree model.

0.36, 0.47, and 0.59, respectively. The S^2 values for the C1′−H1′ terminal residues (G1, T12, A13, and C24) are 0.63, 0.54, 0.58, and 0.63, respectively.

The order parameters of the deoxycytidines are on average smaller than those for the other nucleotides. Interestingly, residue C6 (the methylation site) has the lowest S^2 values (0.65 for C1′−H1′ and 0.57 for C3′−H3′) of all residues, indicating the presence of the largest extent of fast internal motions for this residue. Unlike the earlier comparison of $T_{1\rho}$ and NOE values, the model-free analysis did not suggest that the deoxythymidines are more flexible that other nucleotides.

Table 3: Order Parameters for Ribose Resonances in the *Hha*I DNA Extracted from the ModelFree Analysis

	C1′ S^2	C1′ (model)	C3′ S^2	C3′ (model)
G1	0.63	5	0.49	4
G2	0.84	4	0.79	4
T3	0.72	5	0.73	4
A4	0.86	5	0.83	4
G5	0.74	4	0.79	4
C6	0.65	4	0.57	4
G7	0.68	5		
C8	0.74	5	0.75	4
T9	0.83	2	0.66	4
A10	0.75	5	0.73	4
T11	0.85	2	0.67	4
T12	0.54	5	0.36	5
A13	0.48	5	0.60	2
A14	0.85	2	0.65	4
C23	0.74	4	0.68	4
C24	0.63	4	0.47	5

DISCUSSION

The ability of DNA to undergo substantial conformational changes in response to protein binding or solvent conditions is well-documented, yet just a handful of studies of DNA dynamics at the residue level using NMR relaxation techniques have been reported (*11, 16, 30, 32–34*). Thus, it remains to be investigated whether the intrinsic motional properties of certain DNA sequences contribute to their propensity to undergo sequence-dependent conformational changes.

One the most biologically interesting and dramatic examples of changes in DNA structure in response to protein binding is the flipping out of nucleobases in the active site of methyltransferases (*3*). In seeking to understand the

dynamic properties of DNA that underlie these remarkable conformational changes, we have observed sequence-dependent microsecond to nanosecond dynamics in the DNA sequence recognized by the *Hha*I methylase using solid-state NMR (*7, 35*). In this work, we have systematically probed the motional properties in solution for every residue of the double-stranded DNA target of the *Hha*I methyltransferase by measuring ^{13}C relaxation parameters for both base and sugar resonances. The analyses of the data confirmed that the terminal base-paired residues (G1-C24 and T12-A13) display motions consistent with the presence of fast (picosecond to nanosecond) motions (e.g., reduced S^2), likely due to fraying of the bases at the end of the helix. We also observe that the riboses for deoxycytidines experience an increased level of motion on a faster time scale (picoseconds to nanoseconds) than the other nucleotides in the sequence. It is particularly interesting that the ribose of the cytosine at the methylation site is the most mobile of all. Our results also demonstrate that a majority of the dG and dC base residues within the methylase recognition sequence (GCGC) experience motions on a much slower (microsecond) time scale. Together with the previously reported solid-state NMR studies, these results reveal extensive motions over the entire picosecond to millisecond motional window.

Ribose Dynamics. The first significant observation from our studies is that deoxycytidine C2′−H2″ and C3′−H3′ resonances have higher $T_{1\rho}$ values than other residues. Consistent with this result, ModelFree analysis yields lower-than-average order parameters (S^2 values) for the C3′−H3′ resonance. Both results demonstrate that these residues experience an increased level of motion on the picosecond to nanosecond time scale, compared to other nucleotides. When the C1′−H1′ resonances are examined, both deoxycytidines and deoxythymidine residues have larger transverse relaxation times than purines; the quantitative analysis using ModelFree demonstrates a decrease in order parameters for the C1′−H1′ resonance of the deoxycytidines. Two of the four cytosines are within the GCGC sequence recognized by the methylase, and the other two are at or near the very end of the helix, where fraying is observed. Thus, the cytosines within the *Hha*I recognition sequence GCGC experience increased mobility, the methylase target C6 being the most mobile of all residues.

Consistent with the observation of increased dynamics for the riboses of the cytosines in the sequence, solid-state NMR using static deuterium line shapes and inversion recovery studies of the relaxation properties of the furanose region (2′/2″) of a slightly different *Hha*I target DNA construct, $[d(G_1A_2T_3A_4G_5C_6G_7C_8T_9A_{10}T_{11}C_{12})]_2$, also reported motional differences in the deoxycytidines compared to other residues (*7*). The furanose line shape and relaxation data for the deoxycytidine nucleotides C6 and C8 show clear evidence of dynamic averaging. The line shapes of the deoxycytidines were most strongly perturbed from what is expected for a rigid nucleotide, and the powder-averaged spin lattice relaxation data for 2″ deuterons revealed the shortest $\langle T_{1Z}\rangle$ relaxation times for C6 and C8 (20−30 ms). These differences are dramatic: the $\langle T_{1Z}\rangle$ values for the other nucleotides range from 60 to 80 ms. These variations in dynamics are more subtle in solution relaxation experiments because the motions responsible for modulation of the solid-state line shapes likely occur on time scales that are longer than the rate of molecular rotations and are not easily discernible in solution NMR relaxation experiments.

Are the Motions Observed for the Riboses Specific to the HhaI Recognition Sequence? The solution and solid-state NMR results demonstrate that the riboses of the cytosine within the *Hha*I recognition sequence are dynamic, raising the question of whether these motions are specific to this sequence and therefore potentially part of the mechanism by which the methylase flips off the target cytidine.

There are no solid-state data for the deoxycytidine outside of this region, and the terminal residue would be anomalous anyway because of the motions related to fraying of the helix-terminal base pairs. However, a few other studies measuring the carbon relaxation properties of DNA riboses have also been reported (*11, 32–34*). For the sequence $d(C_1G_2C_3A_4A_5A_6T_7T_8T_9G_{10}C_{11}G_{12})$ (*32*), increased values (∼12% larger) of the transverse relaxation times were also found for the C3 C1′−H1′ resonance of deoxycytidine compared to deoxyadenosine (A4 and A6) and deoxythymidine (T7, T8, and T9); no data were available for C11. A second well-studied system is the DNA target of the *Eco*RI protein $[d(C_1G_2C_3\downarrow G_4\underline{A_5A_6T_7T_8C_9}G_{10}C_{11}G_{12})]$ (the arrow indicates cleavage, and the recognition sequence is underlined), which has three nonterminal deoxycytidines. The internal dynamics of this system has been studied by both solution and solid-state NMR. Carbon relaxation studies of ribose dynamics (*11*) found increased transverse relaxation times (10−20%), indicative of higher mobility, for the C1′−H1′ resonance of all of the nonterminal deoxycytidines (C3, C9, and C11). For C3′−H3′ and C4′−H4′ resonances, data are available for only the C9 residue, but this residue had relaxation rates that were 20 and 13% larger, respectively, than those of the rest of the sequence. Solid-state deuterium inversion recoveries of the furanose region (2′/2″) of the same DNA confirmed that the deoxycytidines are more dynamic than the other nucleotides (*12, 13, 15*). In these studies, C3 are C9 have the shortest $\langle T_{1Z}\rangle$ relaxation times (between ∼35−40 and 10−15 ms as the hydration level increases) compared to those of other nucleotides. C11, which is isolated from the recognition site, is more dynamic than the rest of the sequence ($\langle T_{1Z}\rangle = 79$ ms) with the exception of G10 (which is base paired to C3). The rest of the sequence has relaxation times that range from 80 to 120 ms (*12, 14*).

Altogether, these studies support our observation that the furanose rings of deoxycytidine residues experience less restricted motion than deoxythymidines or purines. They suggest that these fast picosecond to nanosecond motions also occur in the *Eco*RI restriction system and are not specific to the *Hha*I target site, although the particularly high levels of motions observed for the methylation sites remain anomalous.

Base Dynamics. The analysis of the relaxation times for the bases shows that dG and dC bases (mostly found in the *Hha*I recognition sequence GCGC) have average $T_{1\rho}$ relaxation times (28 and 29 ms, respectively) that are 20% smaller than those of the dA and dT bases (34 and 35 ms, respectively). This difference cannot be explained at all with the large and variable chemical shift anisotropies of the bases (*16, 27, 36*), which is the case for other RNA oligonucleotides (*20, 21, 24, 37*). Instead, they reflect real differences in the motional properties of these bases. Consistent with this conclusion, power dependence studies

revealed that the reduced $T_{1\rho}$ values were the result of motions in the 10−100 μs regime, as reflected by the slight $T_{1\rho}$ spin-lock dependence for all of the dC bases. The spin-lock experiments did not reveal the presence of any slower motions for the dG bases (all of which are base paired to dC), but it is possible that these occur on a time scale that is beyond the limits of the experiments. As far as we are aware, other relaxation studies of double-stranded DNA (*16*) have not shown any differences in dynamics between different bases. For example, the *Eco*RI DNA target shows uniform base motions across the sequence, with the exception of the terminal ends.

CONCLUSION

Recent relaxation studies (*38*) of the free M.*Hha*I protein and of the same protein bound to the cofactor indicate that the active site loop possesses dynamics on the fast (nanosecond to picosecond) time scale and residues near one end of the loop (around residue 100) experience intermediate (microsecond to millisecond) time scale motions, the same ranges of motion detected by us in the free DNA. It is difficult at this time to ascertain whether these DNA motions are specific to the methylase GCGC target sequence and whether they play a role in the recognition process due to the paucity of NMR studies of DNA dynamics. Our results demonstrate that the deoxycytidine ribose moieties are more mobile (nanosecond to picosecond time scale) than other nucleotides, but these motions are also evident in other studies of DNA ribose dynamics for other sequences. Interestingly, all of the nucleotides within the *Hha*I recognition site exhibit anomalous base dynamics; however, further studies of mutated recognition sites and similar sequences are necessary to determine if these dynamics play a role in base recognition and/or base flipping.

REFERENCES

1. Bird, A. (1996) The Relationship of DNA to Cancer. *Cancer Surv. 28*, 87–101.
2. Anderson, J. E. (1996) Restriction endonucleases and modification methylases. *Curr. Opin. Struct. Biol. 3*, 24–30.
3. Klimasauskas, S., Kumar, S., Roberts, R. J., and Cheng, X. (1994) HhaI Mehtyltransferase Flips its Target Base out of the DNA Helix. *Cell 76*, 357–369.
4. Klimasauskus, S., and Roberts, R. (1995) M.Hhai Binds Tightly to Substrates Containing Mismatches at the Target Base. *Nucleic Acids Res. 23*, 1388–1395.
5. O'Gara, M., Horton, J., Roberts, R., and Cheng, X. (1998) Structures of HhaI methyltransferase complexed with substrates containing mismatches at the target base. *Nat. Struct. Biol. 5*, 872–877.
6. Youngblood, B., Buller, F., and Reich, N. (2006) Determinants of Sequence-Specific DNA Methylation: Target Recognition and Catalysis Are Coupled in M.HhaI. *Biochemistry (Moscow, Russ. Fed.) 45*, 15563–15572.
7. Meints, G., Miller, P., Pederson, K., Shajani, Z., and Drobny, G. (2008) Solid-State Nuclear Magnetic Resonance Spectroscopy Studies of Furanose Ring Dynamics in the DNA *Hha*I Binding Site. *J. Am. Chem. Soc. 130*, 7305–7314.
8. Klimasauskas, S., Szyperski, T., Serva, S., and Wüthrich, K. (1998) Dynamic Modes of the Flipped-Out Cytosine during HhaI Methyltransferase-DNA Interactions in Solution. *EMBO J. 17*, 317–324.
9. Lipari, G., and Szabo, A. (1982) Model-Free Approach to the Interpreptaion of Nuclear Magnetic Relaxation in Macromolecules. 1. Theory and Range of Validity. *J. Am. Chem. Soc. 104*, 4546–4559.
10. Lipari, G., and Szabo, A. (1982) Model-Free Approach to the Interpreptaion of Nuclear Magnetic Relaxation in Macromolecules. 2. Analysis of Experimental Results. *J. Am. Chem. Soc. 104*, 4559–4570.
11. Boisbouvier, J., Wu, Z., Ono, A., Kainosho, M., and Bax, A. (2003) Rotational diffusion tensor of nucleic acids from ^{13}C NMR relaxation. *J. Biomol. NMR 27*, 133–142.
12. Hatcher, M. (1996) A Solid-State Deuterium NMR Investigation of the Local Dynamics of Nucleotides in the EcoRI Restriction Endonuclease Binding Site. Ph.D. Thesis, University of Washington, Seattle.
13. Hatcher, M., Mattielo, D., Meints, G., Orban, J., and Drobny, G. (1998) A Solid-State Deuterium NMR Study of the Localized Dynamics at the C9pG10 Step in the DNA Dodecamer [d(CGCGAATTCGCG)]$_2$. *J. Am. Chem. Soc. 120*, 9850–9862.
14. Huang, W., Orban, J., Kinatar, A., Reid, B., and Drobny, G. (1990) A Solid-State Deuterium NMR Study of Furanose Ring Dynamics in [d(CGCGAATTCGCG)]$_2$. *J. Am. Chem. Soc. 112*, 9059–9068.
15. Meints, G. (2000) An Investigation of Local DNA Dynamics in Bacterial Restriction Sites by Solid-State Deuterium NMR. Ph.D. Thesis, University of Washington, Seattle.
16. Ying, J., Grishaev, A., and Bax, A. (2006) Carbon-13 chemical shift anisotropy in DNA bases from field dependence of solution NMR relaxation rates. *Magn. Reson. Chem. 44*, 302–310.
17. Varani, G., Aboul-ela, F., and Allain, F. H.-T. (1996) NMR Investigations of RNA Structure. *Prog. Nucl. Magn. Reson. Spectrosc. 29*, 51–127.
18. Santoro, J., and King, G. C. (1993) A Constant-Time 2D Overbodenhausen Experiment for Inverse Corelation of Isotopically Enriched Species. *J. Magn. Reson. 97*, 202–207.
19. Geen, H., and Freeman, R. (1991) Band-Selective Radiofrequency Pulses. *J. Magn. Reson., Ser. B 93*, 93–141.
20. Shajani, Z., and Varani, G. (2005) ^{13}C NMR Relaxation Studies of RNA Base and Ribose Nuclei Reveal a Complex Pattern of Motions in the RNA Binding Site for Human U1A Protein. *J. Mol. Biol. 349*, 699–715.
21. Shajani, Z., Drobny, G. P., and Varani, G. (2007) Binding of U1A Protein Changes RNA Dynamics as Observed by ^{13}C NMR Relaxation Studies. *Biochemistry 46*, 5875–5883.
22. Farrow, N. A., Muhandiram, R., Singer, A. U., Pascal, S. M., Kay, C. M., Gish, G., Shoelson, S. E., Pawson, T., Forman-Kay, J. D., and Kay, L. E. (1994) Backbone Dynamics of a Free and a Phosphopeptide Complexed Src Homology 2 Domain Studied by ^{15}N NMR Relaxation. *Biochemistry 33*, 5984–6003.
23. Mandel, A. M., Akke, M., and Palmer, A. G. I. (1995) Backbone dynamics of *Escherichia coli* ribonuclease HI: Correlations with structure and function in an active enzyme. *J. Mol. Biol. 246*, 144–163.
24. Duchardt, E., and Schwalbe, H. (2005) Residue specific ribose and nucleobase dynamics of the cUUCGg RNA tetraloop motif by NMR ^{13}C relaxation. *J. Biomol. NMR 32*, 295–308.
25. Chen, J., Brooks, C. L., and Wright, P. E. (2004) Model-free analysis of protein dynamics: Assessment of accuracy and model selection protocols based on molecular dynamics simulation. *J. Mol. NMR 29*, 243–257.
26. Ying, J., Grishaev, A., Bryce, D. L., and Bax, A. (2006) Chemical Shift Tensors of Protonated Base Carbons in Helical RNA from NMR Relaxation and Liquid Crystal Measurements. *J. Am. Chem. Soc. 128*, 11443–11454.
27. Stueber, D., and Grant, D. M. (2002) ^{13}C and ^{15}N Chemical Shift Tensors in Adenosine, Guanosine, Dihydrate, 2′-Deoxythymidine, and Cytidine. *J. Am. Chem. Soc. 124*, 10539–10551.
28. Bryce, D. L., Grishaev, A., and Bax, A. (2005) Measurement of Ribose Carbon Chemical Shift Tensors for A-form RNA by Liquid Crystal NMR Spectroscopy. *J. Am. Chem. Soc. 127*, 7387–7396.
29. Fushman, D., and Cowburn, D. (1999) The effect of noncollinearity of ^{15}N-^{1}H dipolar and ^{15}N CSA tensors and rotational anisotropy on ^{15}N relaxation, CSA/dipolar cross correlation, and TROSY. *J. Biomol. NMR 13*, 139–147.
30. Kojima, C., Ono, A., Kainosho, M., and James, T. (1998) DNA Duplex Dynamics: NMR Relaxation Studies of a Decamer with Uniformly ^{13}C-Labeled Purine Nucleotides. *J. Magn. Reson. 135*, 310–333.
31. Schurr, J. M., Babcock, H. P., and Fujimoto, B. S. (1994) A Test of the Model-Free Formulas. Effects of Anisotropic Rotational Diffusion and Dimerization. *J. Magn. Reson., Ser. B 105*, 211–224.
32. Gaudin, F., Chanteloup, L., Thuong, N. T., and Lancelot, G. (1997) Selectively ^{13}C-Enriched DNA: Dynamics of the C1′H1 and C5′H5′

or C5′H5 Vectors on d(CGCAAATTTGCG)$_2$. *Magn. Reson. Chem. 35*, 561–565.

33. Gaudin, F., Paquet, F., Chanteloup, L., Beau, J. M., Nguyen, T. T., and Lancelot, G. (1995) Selectively C-13 Enriched DNA-Dynamics-Dynamics of the C1′-H1′ Vector in d(CGCAAATTTGCG)$_2$. *J. Biomol. NMR,* 5.
34. Spielmann, H. P. (1998) Dynamics of a Bis-intercalator DNA Complex by ^{1}H-Detected Natural Abundance ^{13}C NMR Spectroscopy. *Biochemistry 37*, 16863–16876.
35. Miller, P. A., Shajani, Z., Meints, G. A., Caplow, D., Goobes, G., Varani, G., and Drobny, G. P. (2006) Contrasting Views of the Internal Dynamics of the HhaI Methyltransferase Target DNA Reported by Solution and Solid-State NMR Spectroscopy. *J. Am. Chem. Soc. 128*, 15970–15971.
36. Tang, P., Santos, R. A., and Harbison, G. S. (1989) NMR studies of Oriented DNA. *Adv. Magn. Reson. 13*, 225–255.
37. Shajani, Z., and Varani, G. (2007) NMR Studies of Dynamics in RNA and DNA by ^{13}C Relaxation. *Biopolymers 86*, 348–359.
38. Zhou, H., Shatz, W., Purdy, M., Dahlquist, F., and Reich, N. (2007) Long-Range Structural and Dynamical Changes Induced by Cofactor Binding in DNA Methyltransferase M.HhaI. *Biochemistry 46*, 7261–7268.

BI7020469